Proceedings of the ASME 2014 Conference on Smart Materials, Adaptive Structures and Intelligent Systems
SMASIS2014
September 8-10, 2014, Newport, Rhode Island, USA

SMASIS2014-7714

FAST AND GLOBALLY CONVERGENT NONLINEAR SYSTEM MODEL FOR 3D MAGNETOSTRICTIVE SYSTEMS

Hafez Tari
Department of Mechanical and Aerospace Engineering,
The Ohio State University,
Columbus, Ohio 43210, USA
Email: tari.1@osu.edu

Marcelo J. Dapino*
Department of Mechanical and Aerospace Engineering,
The Ohio State University,
Columbus, Ohio 43210, USA
Email: dapino.1@osu.edu

ABSTRACT

A globally convergent and fully coupled magnetomechanical model for 3D magnetostrictive systems is presented. In magnetostrictive actuators, magnetic field and stress inputs generate magnetic flux density and strain. We refer to models that follow this scheme as direct models (no relation to the direct magnetomechanical effect). In certain design and control situations, inverse models are necessary in which the magnetic field and stress are found from specified magnetic flux density and strains. This inversion typically involves an iterative procedure, which may be prone to convergence issues. An inverse model approach is proposed for arbitrary magnetostrictive materials. The inversion requirement is a continuous and second order differentiable direct model for any chosen magnetostrictive material. The approach is globally convergent, which makes it ideal for use in finite element frameworks. The premise of the proposed iterative system model is to constitute a recursive correction formula based on second order approximations of a novel scalar error function which allows to achieve a faster convergence rate. A continuation approach is then used to achieve global convergence for arbitrary input parameters. To illustrate, Galfenol is chosen as the magnetostrictive material, and analytical derivations of the Jacobian and Hessian matrices are presented. Finally, the computational efficiency of the proposed approach is shown to compare favorably against existing models.

*Address all correspondence to this author.

NOMENCLATURE

x_i The ith element of vector $\mathbf{x}$.
$[x_1;x_2]$ Column vector $\mathbf{x}$ with elements x_1 and x_2.
A_{ij} The $(i,j)^{th}$ element of matrix $\mathbf{A}$.
$|\mathbf{A}|$ Determinant of matrix $\mathbf{A}$.
$tr(\mathbf{A})$ Trace of matrix $\mathbf{A}$.
$\mathbf{I}$ The 3×3 Identity matrix.
$\mathbb{R}$ The set of the real numbers.
$\times$ Vector cross product operator.
$\cdot$ Vector dot product operator.
^{T} Vector/matrix transpose operator.

1 Introduction

Magnetostrictive materials undergo dimensional changes when exposed to a magnetic field, and exhibit magnetization changes when they experience external stress fields. Two common magnetostrictive materials are terbium-dysprosium-iron and iron-gallium alloys, known commonly as Terfenol-D and Galfenol, respectively. The former has relatively large magnetostriction ($\approx$ 1600 ppm) at a moderate magnetic field ($\approx$ 200 kA/m), making it well suited for actuator designs; see for example Chakrabarti and Dapino [1]. Referring to Ref. [2], Galfenol exhibits moderate magnetostriction ($\approx$ 350 ppm) at low magnetic fields ($\approx$ 8 kA/m); possesses high tensile strength ($\approx$ 500 MPa); and demonstrates limited variation in magnetomechanical properties for temperatures between -20 and 80 °C. If composed of less than 20% gallium, Galfenol retains the machinability and ductility of iron, thus it can easily be produced in

Copyright © 2014 by ASME

sheets or wires; welded, threaded or extruded into unprecedented complex geometries to gain significant load-bearing capabilities. In contrast, Terfenol-D is brittle thus always requiring stress biasing to avoid tension. As per Ref. [3], Galfenol exhibits very low hysteresis, and a high Curie temperature (675 °C). Also, the constituent materials for the production of Galfenol are rather inexpensive. See Atulasimha and Flatau [4] for a review of iron-gallium alloys.

To date, several methods exist to efficiently model the behavior of magnetostrictive materials for arbitrary combination of applied stress and magnetic fields. At one extreme, a phenomenological approach fits a curve or surface to measurement data, which provides efficiency but ignores the underlying physics. At the other extreme, micromagnetic models consider all known energies and are very accurate. Macroscopic models use an intermediate approach by relating the macroscopic response of the material to simplified descriptions of the microscopic behavior. Macroscopic models, therefore, strike a balance between efficiency, accuracy, and predictive capability. The classical macroscopic models are the Preisach model [5], Globus model [6], Jiles-Atherton model [7], and Stoner-Wohlfarth model [8]. Ref. [9] compares these models in detail.

For Terfenol-D, in particular, Carman and Mitrovic [10] formulated a model by expanding the Gibbs free energy in a truncated Taylor series, and found the coefficients experimentally. Later, Zheng and Sun [11] took higher order terms in the expansion into account to improve the applicability of the model for larger magnetic field inputs. Recently, a fully coupled 3D energy-averaged model was presented by Chakrabarti and Dapino [1].

Armstrong [12] proposed an incremental hysteretic magnetoelastic constitutive theory of pseudo-cubic ferromagnetostrictive alloys that can be applied to both Terfenol-D and Galfenol. The bulk magnetization and magnetostriction are the expected values of a large collection of magnetic moments. The probability density function is a Boltzmann distribution, where minimum energy orientations are more probable. The Armstrong model is computationally inefficient, as it searches for global energy minima. Atulasimha et al. [13] improved efficiency by considering only 98 fixed orientations. Evans and Dapino [14] greatly enhanced the previous model by solving for the local minima along only six easy directions of Galfenol. The computational cost of this model was further reduced by Chakrabarti [15]. However, this model is prone to singularities, which can burden computation, especially when the model is integrated into finite element solvers. Tari et al. [16] recently addressed this shortcoming through a reformulation of the model with an exact solution procedure.

In magnetostrictive actuators, magnetic field and stress inputs generate magnetic flux density and strain. The aforementioned models follow this scheme, and we call such models as direct models. However, in certain design and control situations, inverse models are necessary in which the magnetic field and stress are found from specified magnetic flux density and strains. This inversion typically involves an iterative procedure. Chakrabarti and Dapino [17] proposed an inverse model, based on the direct model given in Ref. [15], that describes the full nonlinear coupling in 3D Galfenol transducers. However, this model is susceptible to convergence issues, which is drastically alleviated by the further developments of Deng and Dapino [18].

The premise of the foregoing iterative system models is to constitute recursive correction formulae based on first order approximations of some specified error functions. However, the aim of this paper is to achieve a faster convergence rate by taking second order approximations into account. To do this, we formulate the problem in an optimization framework through defining a novel scalar error function, which allows to effectively incorporate Hessian (matrix of the second order derivatives) of the direct model in the formulation. A continuation approach is then used to achieve global convergence for arbitrary input parameters. The inversion requirement is a continuous and second order differentiable direct model for any chosen magnetostrictive material. The approach is globally convergent, which makes it ideal for use in finite element frameworks. While the method is developed for arbitrary magnetostrictive materials, Galfenol is chosen to illustrate the inverse model, and compact analytical derivations of the Jacobian and Hessian matrices corresponding to the direct model given by Tari et al. [16] are presented. Finally, convergence rate of the proposed approach is compared successfully to that of Deng and Dapino [18] for the chosen material.

The rest of the paper is organized as follows. A globally convergent system model for arbitrary magnetostrictive materials is outlined next. A brief review of a recent direct model for Galfenol is reviewed in Section 3. The derivative terms of this direct model that are required by the inverse model are derived analytically in Section 4, which is followed by a discussion on the proposed model performance. Finally, conclusions are given.

2 Magnetostrictive System Model featuring Continuation

Let $\mathbf{H} = [H_1; H_2; H_3]$ be the magnetic field vector, and $\mathbf{T} = [T_1; T_2; T_3; T_4; T_5; T_6]$ be the symmetric stress tensor written in contracted vector notation with the convention $T_1 = T_{11}$, $T_2 = T_{22}$, $T_3 = T_{33}$, $T_4 = T_{12}$, $T_5 = T_{23}$, and $T_6 = T_{13}$. Let, further, $\mathbf{B}(\mathbf{H},\mathbf{T}) = [B_1; B_2; B_3]$ and $\mathbf{S}(\mathbf{H},\mathbf{T}) = [S_1; S_2; S_3; S_4; S_5; S_6]$ be given continuous and differentiable direct models for, respectively, magnetic flux density and strain vectors, which take magnetic field and stress vectors as input. Finally, let $\mathbf{B}^*$ and $\mathbf{S}^*$ denote any discrete magnetic flux density and strain vectors specified from measurements or finite element simulations.

The goal is to find the unknown magnetic field and stress vectors $\mathbf{H}^*$ and $\mathbf{T}^*$ that give rise to $\mathbf{B}^*$ and $\mathbf{S}^*$. That is, the goal is

Copyright © 2014 by ASME

to find $\mathbf{H}$ and $\mathbf{T}$ that satisfy the equations

$$\begin{bmatrix} \mathbf{B}(\mathbf{H},\mathbf{T}) - \mathbf{B}^* \\ \mathbf{S}(\mathbf{H},\mathbf{T}) - \mathbf{S}^* \end{bmatrix} = 0. \tag{1}$$

Our strategy to solving the foregoing system of equations rests on "continuation", which is an iterative approach that offers global convergence; see Refs. [19, 20] for applications of continuation to kinematic design and analysis of rigid mechanisms. Let us rewrite the foregoing vector of error functions as a homotopy

$$\begin{aligned} &\begin{bmatrix} \mathbf{B}(\mathbf{H},\mathbf{T}) - \mathbf{B}^\tau \\ \mathbf{S}(\mathbf{H},\mathbf{T}) - \mathbf{S}^\tau \end{bmatrix} \triangleq \\ &\quad \begin{bmatrix} \mathbf{B}(\mathbf{H},\mathbf{T}) - ((1-\tau)\mathbf{B}(\mathbf{H}^0,\mathbf{T}^0) + \tau\mathbf{B}^*) \\ \mathbf{S}(\mathbf{H},\mathbf{T}) - ((1-\tau)\mathbf{S}(\mathbf{H}^0,\mathbf{T}^0) + \tau\mathbf{S}^*) \end{bmatrix} = 0, \end{aligned} \tag{2}$$

where $\mathbf{H}^0$ and $\mathbf{T}^0$ are known start solutions, and $\tau \in [0,1]$ is the continuation parameter. The idea of the continuation is to break the problem into a series of more manageable subproblems, and to solve them sequentially. In doing so, the solutions to the previous subproblem is used as the start solutions to the current subproblem. In essence, continuation initiates at the start solutions $\mathbf{H}^0$ and $\mathbf{T}^0$ at $\tau = 0$, and traces the solution curves of $\mathbf{H}(\tau)$ and $\mathbf{T}(\tau)$ as τ is incremented, until $\tau = 1$ at which point the desired solutions $\mathbf{H}^*$ and $\mathbf{T}^*$ are obtained.

To solve each subproblem effectively, we solve the minimization problem

$$\underset{\mathbf{H}\in\mathbb{R}^3,\, \mathbf{S}\in\mathbb{R}^6}{\text{Minimize}} \;\; f(\mathbf{H},\mathbf{T}), \tag{3}$$

where f is the scalar objective error function

$$\begin{aligned} f(\mathbf{H},\mathbf{T}) = &\frac{1}{2} w_b^2 \left[\mathbf{B}(\mathbf{H},\mathbf{T}) - \mathbf{B}^\tau\right]^{\mathrm{T}} \left[\mathbf{B}(\mathbf{H},\mathbf{T}) - \mathbf{B}^\tau\right] \\ &+ \frac{1}{2} w_s^2 \left[\mathbf{S}(\mathbf{H},\mathbf{T}) - \mathbf{S}^\tau\right]^{\mathrm{T}} \left[\mathbf{S}(\mathbf{H},\mathbf{T}) - \mathbf{S}^\tau\right], \end{aligned} \tag{4}$$

where w_b and w_s are weighting factors chosen to effectively combine the error contributions of magnetic flux density and strain, respectively. Expanding f in a second order Taylor's series as

$$\begin{aligned} &f(\mathbf{H}+\Delta\mathbf{H},\mathbf{T}+\Delta\mathbf{T}) \approx \\ &\quad f(\mathbf{H},\mathbf{T}) + \overbrace{\left[\frac{\partial f(\mathbf{H},\mathbf{T})}{\partial \mathbf{H}}; \frac{\partial f(\mathbf{H},\mathbf{T})}{\partial \mathbf{T}}\right]^T}^{[\mathbf{J}^f]^T} [\Delta\mathbf{H};\Delta\mathbf{T}] \\ &\quad + \frac{1}{2}[\Delta\mathbf{H};\Delta\mathbf{T}]^{\mathrm{T}} \overbrace{\begin{bmatrix} \frac{\partial^2 f(\mathbf{H},\mathbf{T})}{\partial\mathbf{H}\partial\mathbf{H}} & \frac{\partial^2 f(\mathbf{H},\mathbf{T})}{\partial\mathbf{H}\partial\mathbf{T}} \\ \frac{\partial^2 f(\mathbf{H},\mathbf{T})}{\partial\mathbf{T}\partial\mathbf{H}} & \frac{\partial^2 f(\mathbf{H},\mathbf{T})}{\partial\mathbf{T}\partial\mathbf{T}} \end{bmatrix}}^{[\mathbf{H}^f]} [\Delta\mathbf{H};\Delta\mathbf{T}], \end{aligned} \tag{5}$$

and minimizing it for the incremental magnetic field and stress vectors $\Delta\mathbf{H}$ and $\Delta\mathbf{T}$, may give a recursive correction formula based on the damped Newton method as

$$[\mathbf{H}(i+1);\mathbf{T}(i+1)] = [\mathbf{H}(i);\mathbf{T}(i)] - \alpha_i [\mathbf{H}^f(i)]^{-1} [\mathbf{J}^f(i)], \tag{6}$$

where i is the iteration index, and $\mathbf{J}^f$ and $\mathbf{H}^f$ are called the Jacobian (gradient vector for 1D inputs) and Hessian matrices, respectively. When the derivative terms are known, the algorithm initiates at given start solutions $\mathbf{H}(0)$ and $\mathbf{T}(0)$, which get corrected at successive iterations, until the algorithm is terminated when the residual error is below a predetermined threshold. At this point, the desired $\mathbf{H}^\tau$ and $\mathbf{T}^\tau$ are obtained for each subproblem.

For convenience, the derivatives in eq. (5) or (6) are derived in indicial where it is assumed that the subscripts $p,q \in \{1,\ldots,3\}$ and $i,j \in \{1,\ldots,6\}$. For brevity, $f(\mathbf{H},\mathbf{T})$, $\mathbf{B}(\mathbf{H},\mathbf{T})$ and $\mathbf{S}(\mathbf{H},\mathbf{T})$ are abbreviated, respectively, as f, $\mathbf{B}$, and $\mathbf{S}$. Accordingly, the first order derivatives are

$$\frac{\partial f}{\partial H_p} = w_h \left(w_b^2 \left[\mathbf{B} - \mathbf{B}^\tau\right]^{\mathrm{T}} \frac{\partial \mathbf{B}}{\partial H_p} + w_s^2 \left[\mathbf{S} - \mathbf{S}^\tau\right]^{\mathrm{T}} \frac{\partial \mathbf{S}}{\partial H_p} \right), \tag{7a}$$

$$\frac{\partial f}{\partial T_i} = w_t \left(w_b^2 \left[\mathbf{B} - \mathbf{B}^\tau\right]^{\mathrm{T}} \frac{\partial \mathbf{B}}{\partial T_i} + w_s^2 \left[\mathbf{S} - \mathbf{S}^\tau\right]^{\mathrm{T}} \frac{\partial \mathbf{S}}{\partial T_i} \right), \tag{7b}$$

and the second order derivative are

Copyright © 2014 by ASME

$$\frac{\partial^2 f}{\partial H_p \partial H_q} = w_h^2 \left(w_b^2 \left[\mathbf{B}-\mathbf{B}^\tau\right]^{\mathrm{T}} \frac{\partial^2 \mathbf{B}}{\partial H_p \partial H_q} + w_b^2 \frac{\partial \mathbf{B}^{\mathrm{T}}}{\partial H_p} \frac{\partial \mathbf{B}}{\partial H_q} + w_s^2 \left[\mathbf{S}-\mathbf{S}^\tau\right]^{\mathrm{T}} \frac{\partial^2 \mathbf{S}}{\partial H_p \partial H_q} + w_s^2 \frac{\partial \mathbf{S}^{\mathrm{T}}}{\partial H_p} \frac{\partial \mathbf{S}}{\partial H_q} \right), \tag{8a}$$

$$\frac{\partial^2 f}{\partial T_i \partial T_j} = w_t^2 \left(w_b^2 \left[\mathbf{B}-\mathbf{B}^\tau\right]^{\mathrm{T}} \frac{\partial^2 \mathbf{B}}{\partial T_i \partial T_j} + w_b^2 \frac{\partial \mathbf{B}^{\mathrm{T}}}{\partial T_i} \frac{\partial \mathbf{B}}{\partial T_j} + w_s^2 \left[\mathbf{S}-\mathbf{S}^\tau\right]^{\mathrm{T}} \frac{\partial^2 \mathbf{S}}{\partial T_i \partial T_j} + w_s^2 \frac{\partial \mathbf{S}^{\mathrm{T}}}{\partial T_i} \frac{\partial \mathbf{S}}{\partial T_j} \right), \tag{8b}$$

$$\frac{\partial^2 f}{\partial H_p \partial T_i} = w_h w_t \left(w_b^2 \left[\mathbf{B}-\mathbf{B}^\tau\right]^{\mathrm{T}} \frac{\partial^2 \mathbf{B}}{\partial H_p \partial T_i} + w_b^2 \frac{\partial \mathbf{B}^{\mathrm{T}}}{\partial H_p} \frac{\partial \mathbf{B}}{\partial T_i} + w_s^2 \left[\mathbf{S}-\mathbf{S}^\tau\right]^{\mathrm{T}} \frac{\partial^2 \mathbf{S}}{\partial H_p \partial T_i} + w_s^2 \frac{\partial \mathbf{S}^{\mathrm{T}}}{\partial H_p} \frac{\partial \mathbf{S}}{\partial T_i} \right), \tag{8c}$$

where w_h and w_t are scaling factors for magnetic field and stress vectors. Note that the derivatives of the direct magnetic flux density and stress models present in the foregoing equations must be known. These terms are material specific, and in the following, we take Galfenol as a case study, and after a brief review of a direct model for Galfenol, the corresponding derivative terms are presented analytically.

3 Review of calculation of 3D magnetostriction and magnetic flux density for Galfenol

Tari et al. [16] recently proposed an exact solution procedure for a reformulation of the discrete energy-averaged model, proposed by Evans and Dapino [14], that computes the macroscopic 3D magnetic flux density $\mathbf{B}$ and strain $\mathbf{S}$ by minimizing the Gibbs free energy that is defined locally about each easy crystallographic direction. Magnetocrystalline (anisotropy), magnetoelastic (magnetomechanical coupling), and magnetic field (Zeeman) energies constitute the Gibbs free energy in the vicinity of the kth easy direction written as

$$\overset{k}{G} = \frac{1}{2}\, \overset{k}{\mathbf{m}} \cdot \mathbf{K}\, \overset{k}{\mathbf{m}} - (K\, \overset{k}{\mathbf{c}} + \mu_0 M_s \mathbf{H}) \cdot \overset{k}{\mathbf{m}} + \overset{k}{K}_0, \quad k \in \pm\{1,\ldots,\frac{r}{2}\}, \tag{9}$$

where K and K_0 are anisotropy energy constants; $\mathbf{m} = [m_1; m_2; m_3]$ is the magnetization direction having unit magnitude; r is the number of easy crystallographic directions ($\mathbf{c}$: the $\langle 100 \rangle$ family of six directions for Galfenol); μ_0 and M_s are, respectively, the vacuum permeability and saturation magnetization; and the magnetic stiffness matrix is given by

$$\mathbf{K} = -3 \begin{bmatrix} \lambda_{100} T_1 & \lambda_{111} T_4 & \lambda_{111} T_6 \\ \lambda_{111} T_4 & \lambda_{100} T_2 & \lambda_{111} T_5 \\ \lambda_{111} T_6 & \lambda_{111} T_5 & \lambda_{100} T_3 \end{bmatrix}, \tag{10}$$

where λ_{100} and λ_{111} are magnetostriction constants.

The macroscopic 3D magnetic flux density and strain vectors are defined as weighted sums of the response due to the r minimum energy directions as

$$\mathbf{B} = \mu_0(\mathbf{H} + \overline{\mathbf{M}}) = \mu_0(\mathbf{H} + M_s \sum_{k=\pm 1}^{\pm r/2} \overset{k}{\overline{\xi}}_{hys} \overset{k}{\mathbf{m}}), \tag{11}$$

$$\mathbf{S} = \mathbf{s}\mathbf{T} + \overline{\boldsymbol{\lambda}} = \mathbf{s}\mathbf{T} + \sum_{k=\pm 1}^{\pm r/2} \overset{k}{\overline{\xi}}_{hys} \overset{k}{\boldsymbol{\lambda}}, \tag{12}$$

where $\overset{k}{\overline{\xi}}_{hys}$ and $\overset{k}{\boldsymbol{\lambda}}$ denote, respectively, the averaged hysteretic volume fraction and the magnetostriction tensor written in vector notation for the kth domain; $\mathbf{s}$ stands for the 6×6 mechanical compliance matrix. Letting Ω be a smoothing factor, the former is calculated as a Boltzman-type, energy-weighted average as

$$\overset{k}{\overline{\xi}}_{hys} = \exp\left(-\frac{\overset{k}{G}}{\Omega}\right) \sum_{n=\pm 1}^{\pm r/2} \exp\left(\frac{\overset{n}{G}}{\Omega}\right), \tag{13}$$

and the magnetostriction tensor components are given as

$$\begin{aligned} \overset{k}{\lambda}_{uu} &= \frac{3}{2} \lambda_{100} (\overset{k}{m}_u \overset{k}{m}_u - c_0), \\ \overset{k}{\lambda}_{uv} &= 3\lambda_{111}\, \overset{k}{m}_u \overset{k}{m}_v, \quad u \neq v, \end{aligned} \tag{14}$$

where $u, v \in \{1,2,3\}$, and c_0 is a nondimensional stiffness parameter.

The unit magnitude, minimum energy directions $\overset{k}{\mathbf{m}}$ are calculated from the inhomogeneous eigenvalue problem

$$(\mathbf{K} - \overset{k}{\gamma}\, \mathbf{I})\, \overset{k}{\mathbf{m}} = K\, \overset{k}{\mathbf{c}} + \mu_0 M_s \mathbf{H}, \tag{15a}$$

$$\overset{k}{\mathbf{m}} \cdot \overset{k}{\mathbf{m}} = 1, \tag{15b}$$

Copyright © 2014 by ASME

where $\overset{k}{\gamma}$ is the unknown Lagrange multiplier corresponding to the kth minimum energy direction.

Letting $\mathbf{Q}$ be the orthogonal matrix containing the eigenvectors of $\mathbf{K}$ (with the eigenvalues λ_1, λ_2, and λ_3), Tari et al. [16] reported that

$$\overset{k}{\mathbf{m}} = \mathbf{Q} \begin{bmatrix} \frac{1}{\lambda_1 - \overset{k}{\gamma}} & 0 & 0 \\ 0 & \frac{1}{\lambda_2 - \overset{k}{\gamma}} & 0 \\ 0 & 0 & \frac{1}{\lambda_3 - \overset{k}{\gamma}} \end{bmatrix} \mathbf{Q}^{\mathrm{T}} (K \overset{k}{\mathbf{c}} + \mu_0 M_s \mathbf{H}), \tag{16}$$

where $\overset{k}{\gamma}$ is obtained from the sixth order polynomial:

$$\begin{aligned} &\overset{k}{\bar{\gamma}}{}^6 + 2(\bar{\lambda}_2 + \bar{\lambda}_3)\overset{k}{\bar{\gamma}}{}^5 + \left(\bar{\lambda}_2^2 + 4\bar{\lambda}_2\bar{\lambda}_3 + \bar{\lambda}_3^2 - \bar{Q}_1 \right. \\ &\left. -\bar{Q}_2 - \bar{Q}_3\right)\overset{k}{\bar{\gamma}}{}^4 + 2\left(\bar{\lambda}_2^2\bar{\lambda}_3 + \bar{\lambda}_2\bar{\lambda}_3^2 - \bar{\lambda}_2\bar{Q}_1 \right. \\ &\left. -\bar{\lambda}_3\bar{Q}_1 - \bar{\lambda}_3\bar{Q}_2 - \bar{\lambda}_2\bar{Q}_3\right)\overset{k}{\bar{\gamma}}{}^3 + \left(\bar{\lambda}_2^2\bar{\lambda}_3^2 - \bar{\lambda}_2^2\bar{Q}_1 \right. \\ &\left. -4\bar{\lambda}_2\bar{\lambda}_3\bar{Q}_1 - \bar{\lambda}_3^2\bar{Q}_1 - \bar{\lambda}_3^2\bar{Q}_2 - \bar{\lambda}_2^2\bar{Q}_3\right)\overset{k}{\bar{\gamma}}{}^2 \\ &-2\bar{\lambda}_2\bar{\lambda}_3\bar{Q}_1\left(\bar{\lambda}_2 + \bar{\lambda}_3\right)\overset{k}{\bar{\gamma}} - \bar{\lambda}_2^2\bar{\lambda}_3^2\bar{Q}_1 = 0, \end{aligned} \tag{17}$$

with $\overset{k}{\bar{\gamma}} = \lambda_1 - \overset{k}{\gamma}$, $\bar{\lambda}_2 = \lambda_2 - \lambda_1$, $\bar{\lambda}_3 = \lambda_3 - \lambda_1$, and $[\sqrt{\bar{Q}_1}; \sqrt{\bar{Q}_2}; \sqrt{\bar{Q}_3}]^{\mathrm{T}} = \mathbf{Q}^{\mathrm{T}}(K \overset{k}{\mathbf{c}} + \mu_0 M_s \mathbf{H})$. When eq. (17) has multiple real solutions, the one that results in the lowest Gibbs energy is selected.

4 Derivative terms for the direct model for Galfenol

This section presents analytical derivations of the Jacobian and Hessian terms for the direct model given in the previous section for Galfenol. Note that the same indicial notation, as before, is adopted.

4.1 Jacobian terms

The Jacobian terms can be obtained from differentiating eqs. (11) and (12) with respect to H_p and T_i as

$$\frac{\partial \mathbf{B}}{\partial H_p} = \mu_0 \overset{p}{\mathbf{e}} + \mu_0 M_s \sum_{k=\pm 1}^{\pm r/2} \left(\frac{\partial \overset{k}{\bar{\xi}}_{hys}}{\partial H_p} \overset{k}{\mathbf{m}} + \overset{k}{\bar{\xi}}_{hys} \frac{\partial \overset{k}{\mathbf{m}}}{\partial H_p} \right), \tag{18a}$$

$$\frac{\partial \mathbf{B}}{\partial T_i} = \mu_0 M_s \sum_{k=\pm 1}^{\pm r/2} \left(\frac{\partial \overset{k}{\bar{\xi}}_{hys}}{\partial T_i} \overset{k}{\mathbf{m}} + \overset{k}{\bar{\xi}}_{hys} \frac{\partial \overset{k}{\mathbf{m}}}{\partial T_i} \right), \tag{18b}$$

and

$$\frac{\partial \mathbf{S}}{\partial H_p} = \sum_{k=\pm 1}^{\pm r/2} \frac{\partial \overset{k}{\bar{\xi}}_{hys}}{\partial H_p} \overset{k}{\boldsymbol{\lambda}} + \sum_{k=\pm 1}^{\pm r/2} \overset{k}{\bar{\xi}}_{hys} \frac{\partial \overset{k}{\boldsymbol{\lambda}}}{\partial H_p}, \tag{19a}$$

$$\frac{\partial \mathbf{S}}{\partial T_i} = \mathbf{s}\, \overset{i}{\mathbf{e}} + \sum_{k=\pm 1}^{\pm r/2} \frac{\partial \overset{k}{\bar{\xi}}_{hys}}{\partial T_i} \overset{k}{\boldsymbol{\lambda}} + \sum_{k=\pm 1}^{\pm r/2} \overset{k}{\bar{\xi}}_{hys} \frac{\partial \overset{k}{\boldsymbol{\lambda}}}{\partial T_i}, \tag{19b}$$

where $\overset{p}{\mathbf{e}}$ and $\overset{i}{\mathbf{e}}$ are, respectively, 3- and 6-dimensional unit vectors with one as their p^{th} and i^{th} components.

The derivatives of the averaged hysteretic volume fractions occurring in eqs. (18) and (19) are found upon differentiating eq. (13) with respect to field and stress, respectively, and simplifying the results as

$$\frac{\partial \overset{k}{\bar{\xi}}_{hys}}{\partial H_p} = \frac{\mu_0}{\Omega} \overset{k}{\bar{\xi}}_{hys} \left(M_s \overset{k}{m}_p - \overline{M}_p \right), \tag{20a}$$

$$\frac{\partial \overset{k}{\bar{\xi}}_{hys}}{\partial T_i} = \frac{1}{\Omega} \overset{k}{\bar{\xi}}_{hys} \left(\overset{k}{\lambda}_i - \overline{\lambda}_i \right). \tag{20b}$$

The remaining derivative terms in eq. (18) can be obtained by differentiating the inhomogeneous eigenvalue problem (15) with respect to field and stress, and solving the resulting equations as

$$\frac{\partial \overset{k}{\mathbf{m}}}{\partial H_p} = [\mathbf{K} - \overset{k}{\gamma}\mathbf{I}]^{-1} \left(\frac{\partial \overset{k}{\gamma}}{\partial H_p} \overset{k}{\mathbf{m}} + \mu_0 M_s \overset{p}{\mathbf{e}} \right), \tag{21a}$$

$$\frac{\partial \overset{k}{\mathbf{m}}}{\partial T_i} = [\mathbf{K} - \overset{k}{\gamma}\mathbf{I}]^{-1} \left(\frac{\partial \overset{k}{\gamma}}{\partial T_i} \overset{k}{\mathbf{m}} - \frac{\partial \mathbf{K}}{\partial T_i} \overset{k}{\mathbf{m}} \right), \tag{21b}$$

where

Copyright © 2014 by ASME

$$\frac{\partial \overset{k}{\gamma}}{\partial H_p} = -\mu_0 M_s \frac{\overset{p}{\mathbf{e}} \cdot [\mathbf{K} - \overset{k}{\gamma}\mathbf{I}]^{-1} \overset{k}{\mathbf{m}}}{\overset{k}{\mathbf{m}} \cdot [\mathbf{K} - \overset{k}{\gamma}\mathbf{I}]^{-1} \overset{k}{\mathbf{m}}}, \tag{22a}$$

$$\frac{\partial \overset{k}{\gamma}}{\partial T_i} = \frac{\frac{\partial \mathbf{K}}{\partial T_i} \overset{k}{\mathbf{m}} \cdot [\mathbf{K} - \overset{k}{\gamma}\mathbf{I}]^{-1} \overset{k}{\mathbf{m}}}{\overset{k}{\mathbf{m}} \cdot [\mathbf{K} - \overset{k}{\gamma}\mathbf{I}]^{-1} \overset{k}{\mathbf{m}}}. \tag{22b}$$

Following a simplification procedure, the foregoing results can be combined as

$$\frac{\partial \overset{k}{\mathbf{m}}}{\partial H_p} = -\mu_0 M_s \overset{k}{\Gamma} \overset{k}{\mathbf{m}} \times \left[[\mathbf{K} - \overset{k}{\gamma}\mathbf{I}] (\overset{k}{\mathbf{m}} \times \overset{p}{\mathbf{e}}) \right], \tag{23a}$$

$$\frac{\partial \overset{k}{\mathbf{m}}}{\partial T_i} = \overset{k}{\Gamma} \overset{k}{\mathbf{m}} \times \left[[\mathbf{K} - \overset{k}{\gamma}\mathbf{I}] (\overset{k}{\mathbf{m}} \times \frac{\partial \mathbf{K}}{\partial T_i} \overset{k}{\mathbf{m}}) \right], \tag{23b}$$

where

$$\overset{k}{\Gamma} = \frac{|\mathbf{K} - \overset{k}{\gamma}\mathbf{I}|^{-1}}{\overset{k}{\mathbf{m}} \cdot [\mathbf{K} - \overset{k}{\gamma}\mathbf{I}]^{-1} \overset{k}{\mathbf{m}}}.$$

Finally, the remaining derivative terms in eq. (19) can be obtained by differentiating eq. (14) with respect to field and stress as

$$\frac{\partial \overset{k}{\lambda}_{uu}}{\partial H_p} = 3\lambda_{100} \overset{k}{m}_u \frac{\partial \overset{k}{m}_u}{\partial H_p},$$
$$\frac{\partial \overset{k}{\lambda}_{uv}}{\partial H_p} = 3\lambda_{111} \left(\overset{k}{m}_u \frac{\partial \overset{k}{m}_v}{\partial H_p} + \overset{k}{m}_v \frac{\partial \overset{k}{m}_u}{\partial H_p} \right), \quad u \neq v, \tag{24a}$$

$$\frac{\partial \overset{k}{\lambda}_{uu}}{\partial T_i} = 3\lambda_{100} \overset{k}{m}_u \frac{\partial \overset{k}{m}_u}{\partial T_i},$$
$$\frac{\partial \overset{k}{\lambda}_{uv}}{\partial T_i} = 3\lambda_{111} \left(\overset{k}{m}_u \frac{\partial \overset{k}{m}_v}{\partial T_i} + \overset{k}{m}_v \frac{\partial \overset{k}{m}_u}{\partial T_i} \right), \quad u \neq v. \tag{24b}$$

4.2 Hessian terms

The Hessian terms can be obtained from differentiating eq. (18) with respect to H_p and T_i as

$$\frac{\partial^2 \mathbf{B}}{\partial H_p \partial H_q} = \mu_0 M_s \sum_{k=\pm 1}^{\pm r/2} \left(\frac{\partial^2 \overset{k}{\xi}_{hys}}{\partial H_p \partial H_q} \overset{k}{\mathbf{m}} + \frac{\partial \overset{k}{\xi}_{hys}}{\partial H_p} \frac{\partial \overset{k}{\mathbf{m}}}{\partial H_q} + \overset{k}{\xi}_{hys} \frac{\partial^2 \overset{k}{\mathbf{m}}}{\partial H_p \partial H_q} + \frac{\partial \overset{k}{\xi}_{hys}}{\partial H_q} \frac{\partial \overset{k}{\mathbf{m}}}{\partial H_p} \right), \tag{25}$$

$$\frac{\partial^2 \mathbf{B}}{\partial T_i \partial T_j} = \mu_0 M_s \sum_{k=\pm 1}^{\pm r/2} \left(\frac{\partial^2 \overset{k}{\xi}_{hys}}{\partial T_i \partial T_j} \overset{k}{\mathbf{m}} + \frac{\partial \overset{k}{\xi}_{hys}}{\partial T_i} \frac{\partial \overset{k}{\mathbf{m}}}{\partial T_j} + \overset{k}{\xi}_{hys} \frac{\partial^2 \overset{k}{\mathbf{m}}}{\partial T_i \partial T_j} + \frac{\partial \overset{k}{\xi}_{hys}}{\partial T_j} \frac{\partial \overset{k}{\mathbf{m}}}{\partial T_i} \right), \tag{26}$$

and

$$\frac{\partial^2 \mathbf{B}}{\partial H_p \partial T_i} = \mu_0 M_s \sum_{k=\pm 1}^{\pm r/2} \left(\frac{\partial^2 \overset{k}{\xi}_{hys}}{\partial H_p \partial T_i} \overset{k}{\mathbf{m}} + \frac{\partial \overset{k}{\xi}_{hys}}{\partial H_p} \frac{\partial \overset{k}{\mathbf{m}}}{\partial T_i} + \overset{k}{\xi}_{hys} \frac{\partial^2 \overset{k}{\mathbf{m}}}{\partial H_p \partial T_i} + \frac{\partial \overset{k}{\xi}_{hys}}{\partial T_i} \frac{\partial \overset{k}{\mathbf{m}}}{\partial H_p} \right), \tag{27}$$

and differentiating eq. (19) with respect to H_p and T_i as

$$\frac{\partial^2 \mathbf{S}}{\partial H_p \partial H_q} = \sum_{k=\pm 1}^{\pm r/2} \left(\frac{\partial^2 \overset{k}{\xi}_{hys}}{\partial H_p \partial H_q} \overset{k}{\boldsymbol{\lambda}} + \frac{\partial \overset{k}{\xi}_{hys}}{\partial H_p} \frac{\partial \overset{k}{\boldsymbol{\lambda}}}{\partial H_q} + \overset{k}{\xi}_{hys} \frac{\partial^2 \overset{k}{\boldsymbol{\lambda}}}{\partial H_p \partial H_q} + \frac{\partial \overset{k}{\xi}_{hys}}{\partial H_q} \frac{\partial \overset{k}{\boldsymbol{\lambda}}}{\partial H_p} \right), \tag{28}$$

Copyright © 2014 by ASME

$$\frac{\partial^2 \mathbf{S}}{\partial T_i \partial T_j} = \sum_{k=\pm 1}^{\pm r/2} \left(\frac{\partial^2 \overset{k}{\overline{\xi}}_{hys}}{\partial T_i \partial T_j} \overset{k}{\boldsymbol{\lambda}} + \frac{\partial \overset{k}{\overline{\xi}}_{hys}}{\partial T_i} \frac{\partial \overset{k}{\boldsymbol{\lambda}}}{\partial T_j} + \overset{k}{\overline{\xi}}_{hys} \frac{\partial^2 \overset{k}{\boldsymbol{\lambda}}}{\partial T_i \partial T_j} + \frac{\partial \overset{k}{\overline{\xi}}_{hys}}{\partial T_j} \frac{\partial \overset{k}{\boldsymbol{\lambda}}}{\partial T_i} \right), \tag{29}$$

and

$$\frac{\partial^2 \mathbf{S}}{\partial H_p \partial T_i} = \sum_{k=\pm 1}^{\pm r/2} \left(\frac{\partial^2 \overset{k}{\overline{\xi}}_{hys}}{\partial H_p \partial T_i} \overset{k}{\boldsymbol{\lambda}} + \frac{\partial \overset{k}{\overline{\xi}}_{hys}}{\partial H_p} \frac{\partial \overset{k}{\boldsymbol{\lambda}}}{\partial T_i} + \overset{k}{\overline{\xi}}_{hys} \frac{\partial^2 \overset{k}{\boldsymbol{\lambda}}}{\partial H_p \partial T_i} + \frac{\partial \overset{k}{\overline{\xi}}_{hys}}{\partial T_i} \frac{\partial \overset{k}{\boldsymbol{\lambda}}}{\partial H_p} \right). \tag{30}$$

The second order derivatives of the averaged hysteretic volume fractions in the foregoing equations may be obtained from differentiating eq. (20) with respect to field and stress as

$$\frac{\partial^2 \overset{k}{\overline{\xi}}_{hys}}{\partial H_p \partial H_q} = \frac{\mu_0}{\Omega} \left(\frac{\partial \overset{k}{\overline{\xi}}_{hys}}{\partial H_q} \left(M_s \overset{k}{m}_p - \overline{M}_p \right) + M_s \overset{k}{\overline{\xi}}_{hys} \frac{\partial \overset{k}{m}_p}{\partial H_q} \right) - \frac{\mu_0 M_s}{\Omega} \overset{k}{\overline{\xi}}_{hys} \sum_{n=\pm 1}^{\pm r/2} \left(\frac{\partial \overset{n}{\overline{\xi}}_{hys}}{\partial H_q} \overset{n}{m}_p + \overset{n}{\overline{\xi}}_{hys} \frac{\partial \overset{n}{m}_p}{\partial H_q} \right), \tag{31}$$

$$\frac{\partial^2 \overset{k}{\overline{\xi}}_{hys}}{\partial T_i \partial T_j} = \frac{1}{\Omega} \left(\frac{\partial \overset{k}{\overline{\xi}}_{hys}}{\partial T_j} \left(\overset{k}{\lambda}_i - \overline{\lambda}_i \right) + \overset{k}{\overline{\xi}}_{hys} \frac{\partial \overset{k}{\lambda}_i}{\partial T_j} \right) - \frac{1}{\Omega} \overset{k}{\overline{\xi}}_{hys} \sum_{n=\pm 1}^{\pm r/2} \left(\frac{\partial \overset{n}{\overline{\xi}}_{hys}}{\partial T_j} \overset{n}{\lambda}_i + \overset{n}{\overline{\xi}}_{hys} \frac{\partial \overset{n}{\lambda}_i}{\partial T_j} \right), \tag{32}$$

and

$$\frac{\partial^2 \overset{k}{\overline{\xi}}_{hys}}{\partial H_p \partial T_i} = \frac{\mu_0}{\Omega} \left(\frac{\partial \overset{k}{\overline{\xi}}_{hys}}{\partial T_i} \left(M_s \overset{k}{m}_p - \overline{M}_p \right) + M_s \overset{k}{\overline{\xi}}_{hys} \frac{\partial \overset{k}{m}_p}{\partial T_i} \right) - \frac{\mu_0 M_s}{\Omega} \overset{k}{\overline{\xi}}_{hys} \sum_{n=\pm 1}^{\pm r/2} \left(\frac{\partial \overset{n}{\overline{\xi}}_{hys}}{\partial T_i} \overset{n}{m}_p + \overset{n}{\overline{\xi}}_{hys} \frac{\partial \overset{n}{m}_p}{\partial T_i} \right). \tag{33}$$

To obtain a most simplified version of the remaining second order derivative terms in eqs. (25)-(27), we differentiate the inhomogeneous eigenvalue problem (15) twice with respect to field and stress, and solve the resulting equations for the emerging intermediate unknowns, and after a detailed simplification procedure, we finally have

$$\frac{\partial^2 \overset{k}{\mathbf{m}}}{\partial H_p \partial H_q} = -\overset{k}{\Gamma} \, |\mathbf{K} - \overset{k}{\gamma} \mathbf{I}| \left(\frac{\partial \overset{k}{\mathbf{m}}}{\partial H_p} \cdot \frac{\partial \overset{k}{\mathbf{m}}}{\partial H_q} \right) [\mathbf{K} - \overset{k}{\gamma} \mathbf{I}]^{-1} \overset{k}{\mathbf{m}} - \overset{k}{\Gamma} \overset{k}{\mathbf{m}} \times [\mathbf{K} - \overset{k}{\gamma} \mathbf{I}] \left(\overset{k}{\mathbf{m}} \times \left[\frac{\partial \overset{k}{\gamma}}{\partial H_p} \frac{\partial \overset{k}{\mathbf{m}}}{\partial H_q} + \frac{\partial \overset{k}{\gamma}}{\partial H_q} \frac{\partial \overset{k}{\mathbf{m}}}{\partial H_p} \right] \right), \tag{34}$$

$$\frac{\partial^2 \overset{k}{\mathbf{m}}}{\partial T_i \partial T_j} = -\overset{k}{\Gamma} \, |\mathbf{K} - \overset{k}{\gamma} \mathbf{I}| \left(\frac{\partial \overset{k}{\mathbf{m}}}{\partial T_i} \cdot \frac{\partial \overset{k}{\mathbf{m}}}{\partial T_j} \right) [\mathbf{K} - \overset{k}{\gamma} \mathbf{I}]^{-1} \overset{k}{\mathbf{m}} + \overset{k}{\Gamma} \overset{k}{\mathbf{m}} \times [\mathbf{K} - \overset{k}{\gamma} \mathbf{I}] \left(\overset{k}{\mathbf{m}} \times \left[[\frac{\partial \mathbf{K}}{\partial T_i} - \frac{\partial \overset{k}{\gamma}}{\partial T_i} \mathbf{I}] \frac{\partial \overset{k}{\mathbf{m}}}{\partial T_j} + [\frac{\partial \mathbf{K}}{\partial T_j} - \frac{\partial \overset{k}{\gamma}}{\partial T_j} \mathbf{I}] \frac{\partial \overset{k}{\mathbf{m}}}{\partial T_i} \right] \right), \tag{35}$$

and

$$\frac{\partial^2 \overset{k}{\mathbf{m}}}{\partial H_p \partial T_i} = -\overset{k}{\Gamma} \, |\mathbf{K} - \overset{k}{\gamma} \mathbf{I}| \left(\frac{\partial \overset{k}{\mathbf{m}}}{\partial H_p} \cdot \frac{\partial \overset{k}{\mathbf{m}}}{\partial T_i} \right) [\mathbf{K} - \overset{k}{\gamma} \mathbf{I}]^{-1} \overset{k}{\mathbf{m}} + \overset{k}{\Gamma} \overset{k}{\mathbf{m}} \times [\mathbf{K} - \overset{k}{\gamma} \mathbf{I}] \left(\overset{k}{\mathbf{m}} \times \left[[\frac{\partial \mathbf{K}}{\partial T_i} - \frac{\partial \overset{k}{\gamma}}{\partial T_i} \mathbf{I}] \frac{\partial \overset{k}{\mathbf{m}}}{\partial H_p} - \frac{\partial \overset{k}{\gamma}}{\partial H_p} \frac{\partial \overset{k}{\mathbf{m}}}{\partial T_i} \right] \right). \tag{36}$$

Finally, the remaining unknown derivative terms in eqs. (28)-(30) are obtained from differentiating eq. (24) with respect to field and stress as

Copyright © 2014 by ASME

$$\frac{\partial^2 \overset{k}{\lambda}_{uu}}{\partial H_p \partial H_q} = 3\lambda_{100}\left(\overset{k}{m}_u \frac{\partial^2 \overset{k}{m}_u}{\partial H_p \partial H_q} + \frac{\partial \overset{k}{m}_u}{\partial H_p}\frac{\partial \overset{k}{m}_u}{\partial H_q}\right),$$
$$\frac{\partial^2 \overset{k}{\lambda}_{uv}}{\partial H_p \partial H_q} = 3\lambda_{111}\left(\overset{k}{m}_u \frac{\partial^2 \overset{k}{m}_v}{\partial H_p \partial H_q} + \frac{\partial \overset{k}{m}_u}{\partial H_p}\frac{\partial \overset{k}{m}_v}{\partial H_q} + \overset{k}{m}_v \frac{\partial^2 \overset{k}{m}_u}{\partial H_p \partial H_q} + \frac{\partial \overset{k}{m}_v}{\partial H_p}\frac{\partial \overset{k}{m}_u}{\partial H_q}\right), \quad u \neq v, \tag{37}$$

$$\frac{\partial^2 \overset{k}{\lambda}_{uu}}{\partial T_i \partial T_j} = 3\lambda_{100}\left(\overset{k}{m}_u \frac{\partial^2 \overset{k}{m}_u}{\partial T_i \partial T_j} + \frac{\partial \overset{k}{m}_u}{\partial T_i}\frac{\partial \overset{k}{m}_u}{\partial T_j}\right),$$
$$\frac{\partial^2 \overset{k}{\lambda}_{uv}}{\partial T_i \partial T_j} = 3\lambda_{111}\left(\overset{k}{m}_u \frac{\partial^2 \overset{k}{m}_v}{\partial T_i \partial T_j} + \frac{\partial \overset{k}{m}_u}{\partial T_i}\frac{\partial \overset{k}{m}_v}{\partial T_j} + \overset{k}{m}_v \frac{\partial^2 \overset{k}{m}_u}{\partial T_i \partial T_j} + \frac{\partial \overset{k}{m}_v}{\partial T_i}\frac{\partial \overset{k}{m}_u}{\partial T_j}\right), \quad u \neq v, \tag{38}$$

and

$$\frac{\partial^2 \overset{k}{\lambda}_{uu}}{\partial H_p \partial T_i} = 3\lambda_{100}\left(\overset{k}{m}_u \frac{\partial^2 \overset{k}{m}_u}{\partial H_p \partial T_i} + \frac{\partial \overset{k}{m}_u}{\partial H_p}\frac{\partial \overset{k}{m}_u}{\partial T_i}\right),$$
$$\frac{\partial^2 \overset{k}{\lambda}_{uv}}{\partial H_p \partial T_i} = 3\lambda_{111}\left(\overset{k}{m}_u \frac{\partial^2 \overset{k}{m}_v}{\partial H_p \partial T_i} + \frac{\partial \overset{k}{m}_u}{\partial H_p}\frac{\partial \overset{k}{m}_v}{\partial T_i} + \overset{k}{m}_v \frac{\partial^2 \overset{k}{m}_u}{\partial H_p \partial T_i} + \frac{\partial \overset{k}{m}_v}{\partial H_p}\frac{\partial \overset{k}{m}_u}{\partial T_i}\right), \quad u \neq v. \tag{39}$$

5 Inverse model performance

No other inverse model corresponding to the direct model that is reviewed in Section 3 has been reported in the literature. However, for a slightly different direct model, i.e. that of Ref. [15], Deng and Dapino [18] proposed an inverse model, which is based on the quasi-Newton method. To gain a sense of performance of the proposed inverse model, we compare its rate of convergence against that of Deng and Dapino [18], but provide no timing information since the direct models are of different formulations. See Ref. [16] for details. For a fair comparison, we set the continuation parameter τ to one in the proposed model, so as to disable continuation.

To generate comparative data, magnetic field and stress spaces are specified, with the constraint that the sampled stress tensor must have a von Mises stress smaller than 500 MPa, which is a rough estimate of the ultimate strength of Galfenol. Each space is discretized and fed to the direct model given in Section 3, to produce magnetic induction and strain spaces. To benchmark the inverse models, these datasets are fed to the inverse models to see whether the original magnetic field and stress inputs are returned up to a tolerance of 10^{-9}.

As for the direct model parameters, Evans [14] collected magnetic induction and strain measurements, for uniaxial actuation and sensing, of textured $Fe_{81.5}Ga_{18.5}$ grown in $\langle 100 \rangle$ along the rod axis with the Free Stand Zone Melt method (FSZM) at Etrema Products Inc. For this dataset, Tari et al. reported the direct model parameters, which are tabulated in Table 1.

TABLE 1: Parameters for the direct model, given in Section 3, for $\langle 100 \rangle$ $Fe_{81.5}Ga_{18.5}$ grown with FSZM (Tari et al. [16]).

Par.	M_s (kA/m)	E (GPa)	λ_{100} (ppm)	λ_{111} (ppm)
Value	1242.20	74.49	172.31	0.00
Par.	c_0	K (kJ/m^3)	K_{100} (J/m^3)	Ω (J)
Value	0.38	35.58	412.18	1330.00

Figure 1 illustrates the direct and inverse model simulations for 1D magnetic field and stress inputs. The solid curves on sub-figures (a,b) and (d,e) represent the direct model simulations for actuation and sensing cases, respectively. As explained above, equally spaced points are chosen on these curves, and are fed to the two inverse models, i.e. the proposed model and the existing model by Deng and Dapino [18].

Sub-figures 1 (c) and (f) depict the maximum number of iterations that the two inverse models take, respectively, at constant magnetic field and stress states. Both the existing and proposed inverse models are able to solve the inverse magnetomechanical problem effectively. Nonetheless, the existing approach has a few failures for this 1D case. In addition, the proposed approach converges in fewer iterations than the existing approach. This faster rate of convergence is expected, as the proposed model employs exact derivative terms, while the existing approach employs approximate terms, development of which is a premise of the quasi-Newton method.

It is worth indicating that, for a 1D case and at constant stress values, an ideal inversion procedure must be independent of the sign of the field inputs. This is demonstrated in sub-figure 1 (c),

Copyright © 2014 by ASME

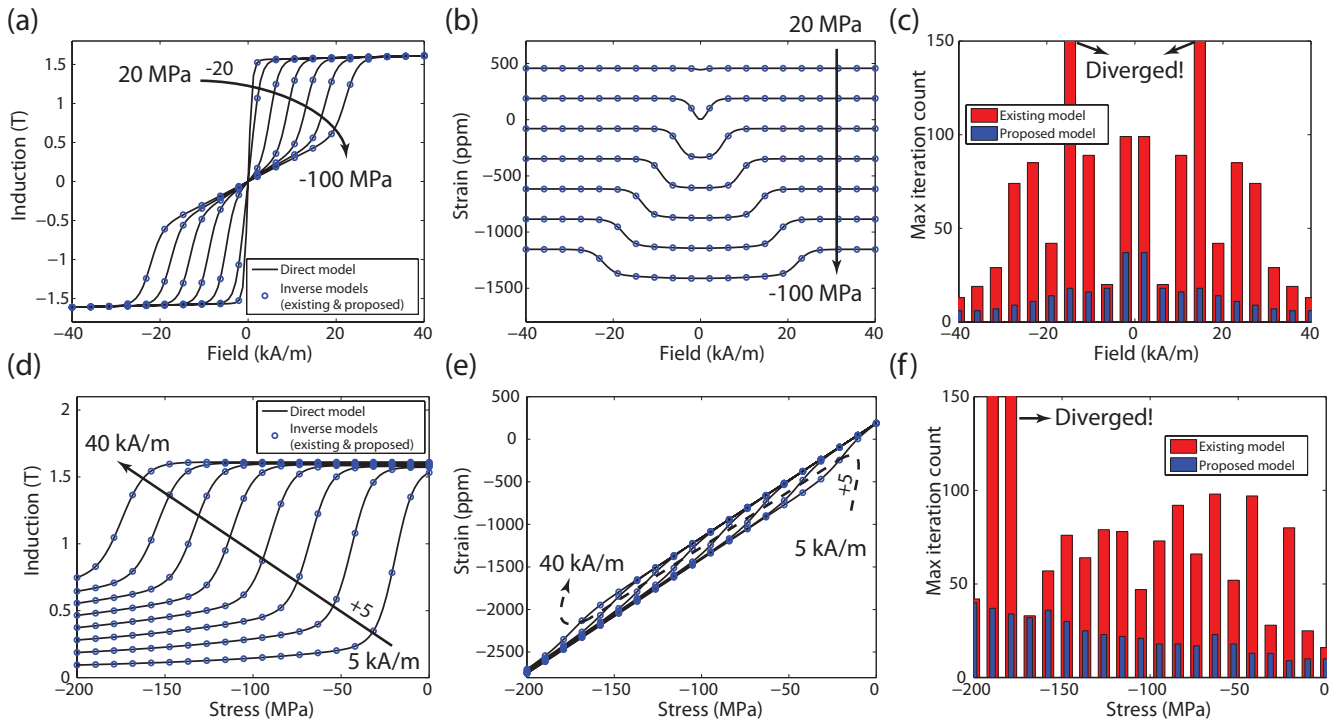

FIGURE 1: Direct and inverse model simulations for $\langle 100 \rangle$ $Fe_{81.5}Ga_{18.5}$ grown with FSZM for 1D (a,b,c) actuation, and (d,e,f) sensing. The existing inverse model is that of Deng and Dapino [18].

as the iteration counts for both inversion models are symmetric about the origin.

5.1 Choice of the iterative step size α

For both the quasi-Newton method and the damped Newton method, the step size α, present for example in eq. (6), must be calculated at each iteration. There is a variety of line search algorithms for this purpose, but they fall into two major categories: exact and approximate. For the simulations, an exact line search based on Golden Section Search (see, for example, Ref. [21]) is used. However, an approximate line search is often sufficient, and can save much computational time. This will be the subject of future work.

5.2 Choice of start solution

Start solutions have a major role in the success of iterative techniques, such as quasi- or damped Newton methods. Even if chosen within the convergence zone, an ill-conditioned start solution may lead to a long runtime. As shown in previous sections, the exact derivative terms, even if compact, are unwieldy, and computationally expensive to evaluate. Even if they lead to minimal number of iterations, they are most efficient when used for local rather than global convergence. Therefore, it is more efficient to carry on a preprocessing step in which a less robust but faster approach such as quasi-Newton method is used to generate a reasonable approximate solution. Then, feeding this solution as a start solution to the main algorithm would save computational time. Alternatively, one may use continuation, which is self-constructive, as it automatically generates a reasonably well-conditioned start solution through solving a series of intermediate sub-problems.

For the simulations, zero start solutions are used. However, the inverse model is devised for use in a finite element framework. In such a case, the system state is known at some instant, and this state is a good candidate as a start solution for the next state. This feature is useful for control applications.

6 Conclusions

In certain design and control situations, inverse models are necessary in which the magnetic field and stress are found from specified magnetic flux density and strains. This inversion typically involves an iterative procedure, which may be prone to convergence issues.

In this paper, a fully coupled magnetomechanical system model for arbitrary magnetostrictive materials was presented. The model requirement is a continuous and second order differentiable direct model for any chosen magnetostrictive material. The approach is globally convergent, which makes it ideal for

Copyright © 2014 by ASME

use in finite element frameworks. The premise of the existing iterative system models is to constitute recursive correction formulae based on first order approximations of some specified error functions. However, to achieve a faster convergence rate, we formulated the problem in an optimization framework through defining a novel scalar error function, and took second order approximations into account. A continuation approach was then developed to achieve global convergence for arbitrary input parameters.

The inverse model is valid for arbitrary magnetostrictive materials. To illustrate, Galfenol was chosen as the magnetostrictive material, and fully compact analytical derivations of the Jacobian and Hessian matrices were presented. The convergence rate of the proposed approach was compared successfully to an existing system model, which is based on quasi-Newton method. An efficient line search algorithm and a carefully developed start solution are needed. As for the latter, start solutions are obviated when using continuation, which generates them automatically. Alternatively, when using the model in a finite element framework, the current system state can be used as a reasonable candidate for the start solution.

ACKNOWLEDGMENT

The authors wish to acknowledge the financial support from NASA Glenn Research Center and Honda R&D Americas through the Smart Vehicle Concepts Center (www.SmartVehicleCenter.org) at the Ohio State University.

REFERENCES

[1] Chakrabarti, S., and Dapino, M. J., 2012. "Fully coupled discrete energy-averaged model for Terfenol-D". *Journal of Applied Physics,* ***111***(5).

[2] Kellogg, R. A., 2003. "Development and modeling of iron–gallium alloys". Ph.D. Dissertation, Iowa State University.

[3] Jayaraman, T. V., Srisukhumbowornchai, N., Guruswamy, S., and Free, M. L., 2007. "Corrosion studies of single crystals of iron-gallium alloys in aqueous environments". *Corrosion Science,* ***49***(10), pp. 4015–4027.

[4] Atulasimha, J., and Flatau, A. B., 2011. "A review of magnetostrictive irongallium alloys". *Smart Materials and Structures,* ***20***(4), p. 043001.

[5] Preisach, F., 1935. "Über die magnetische nachwirkung". *Zeitschrift für Physik,* ***94***(5–6), pp. 277–302.

[6] Globus, A., 1975. "Universal hysteresis loop for soft ferrimagnetic material". *Proc. Europ. Physical Society, Conference on Soft Magnetic Material,* ***2***, p. 233.

[7] Jiles, D. C., and Atherton, D. L., 1986. "Theory of ferromagnetic hysteresis". *Journal of Magnetism and Magnetic Materials,* ***61***, pp. 48–60.

[8] Stoner, E. C., and Wohlfarth, E. P., 1991. "A mechanism of magnetic hysteresis in heterogeneous alloys". *IEEE Transactions on Magnetics,* ***27***(4), pp. 3475–3518.

[9] Liorzou, F., Phelps, B., and Atherton, D. L., 2000. "Macroscopic models of magnetization". *IEEE Transactions on Magnetics,* ***36***(2), pp. 418–428.

[10] Carman, G. P., and Mitrovic, M., 1995. "Nonlinear constitutive relations for magnetostrictive materials with applications to 1-D problems". *Journal of Intelligent Material Systems and Structures,* ***6***(5), pp. 673–683.

[11] Zheng, X. J., and Sun, L., 2006. "A nonlinear constitutive model of magneto-thermo-mechanical coupling for giant magnetostrictive materials". *Journal of Applied Physics,* ***100***(6).

[12] Armstrong, W. D., 2003. "An incremental theory of magneto-elastic hysteresis in pseudo-cubic ferromagnetostrictive alloys". *Journal of Magnetism and Magnetic Materials,* ***263***, pp. 208–218.

[13] Atulasimha, J., Akhras, G., and Flatau, A. B., 2008. "Comprehensive three dimensional hysteretic magnetomechanical model and its validation with experimental ¡110¿ single-crystal iron-gallium behavior". *Journal of Applied Physics,* ***103***(7), p. 07B336.

[14] Evans, P., and Dapino, M., 2010. "Efficient magnetic hysteresis model for field and stress application in magnetostrictive Galfenol". *Journal of Applied Physics,* ***107***(6), p. 063906.

[15] Chakrabarti, S., 2011. "Modeling of 3D magnetostrictive systems with application to Galfenol and Terfenol-D transducers". Ph.D. Dissertation, The Ohio State University.

[16] Tari, H., Scheidler, J. J., and Dapino, M. J., 2014. "Robust solution procedure for the discrete energy-averaged model on calculation of the 3d hysteretic magnetization and magnetostriction of iron-gallium alloys". *Journal of Applied Physics, In review*.

[17] Chakrabarti, S., and Dapino, M. J., 2011. "Nonlinear finite element model for 3D Galfenol systems". *Smart Materials and Structures,* ***20***(10), p. 105034.

[18] Deng, Z., and Dapino, M. J., 2013. "Characterization and finite element modeling of galfenol minor flux density loops". *Proc. SPIE, Behavior and Mechanics of Multifunctional Materials and Composites,* ***8689***, pp. 86890V–11.

[19] Tari, H., and Su, H. J., 2010. "Complete solution to the eight-point path generation of slider-crank four-bar linkages". *Journal of Mechanical Design,* ***132***(8), p. 081003.

[20] Tari, H., Su, H. J., and Li, T. Y., 2010. "A constrained homotopy technique for excluding unwanted solutions from polynomial equations arising in kinematics problems". *Mechanism and Machine Theory,* ***45***(6), pp. 898–910.

[21] M. J. Box, D. Davies, W. H. S., 1969. *Nonlinear Optimization Techniques (Monograph No. 5: Mathematical and Statistical Techniques for Industry).* Imperial Chemical In-

Copyright © 2014 by ASME

dustries Limited, Oliver & Boyd.

A Detailed derivation of a selection of the Derivative Terms

The derivatives of the Gibbs free energy (eq. (9)) have major roles in the analytical reduction of the derivation of the subsequent derivative terms, which have already been presented in the foregoing sections. Therefore, a step by step derivation procedure for such key terms is given as follows.

First, we rewrite the Gibbs free energy given by eq. (9) as

$$\begin{aligned} \overset{k}{G} = & \frac{1}{2}\,\overset{k}{\mathbf{m}}\cdot\mathbf{K}\,\overset{k}{\mathbf{m}} - (K\,\overset{k}{\mathbf{c}} + \mu_0 M_s \mathbf{H})\cdot\overset{k}{\mathbf{m}} + \overset{k}{K}_0 \\ & + \frac{3}{2} c_0 \lambda_{100}\, tr(\mathbf{T}), \quad k \in \pm\{1,\ldots,\frac{r}{2}\}, \end{aligned} \tag{40}$$

which leaves the direct model unchanged, as we are shifting the base energy of all of the easy axes the same amount. Differentiating the foregoing equation with respect to field and stress gives

$$\begin{aligned} \frac{\partial\,\overset{k}{G}}{\partial H_p} &= \frac{\partial\overset{k}{\mathbf{m}}}{\partial H_p}\cdot\mathbf{K}\,\overset{k}{\mathbf{m}} - \mu_0 M_s m_p - (K\,\overset{k}{\mathbf{c}} + \mu_0 M_s \mathbf{H})\cdot\frac{\partial\overset{k}{\mathbf{m}}}{\partial H_p} \\ &= \frac{\partial\overset{k}{\mathbf{m}}}{\partial H_p}\cdot(\mathbf{K}\,\overset{k}{\mathbf{m}} - K\,\overset{k}{\mathbf{c}} - \mu_0 M_s \mathbf{H}) - \mu_0 M_s m_p \\ &= \overset{k}{\gamma}\,\frac{\partial\overset{k}{\mathbf{m}}}{\partial H_p}\cdot\overset{k}{\mathbf{m}} - \mu_0 M_s m_p = -\mu_0 M_s m_p, \end{aligned} \tag{41}$$

and

$$\begin{aligned} \frac{\partial\,\overset{k}{G}}{\partial T_i} &= \frac{\partial\,\overset{k}{\mathbf{m}}}{\partial T_i}\cdot\mathbf{K}\,\overset{k}{\mathbf{m}} + \frac{1}{2}\,\overset{k}{\mathbf{m}}\cdot\frac{\partial\mathbf{K}}{\partial T_i}\,\overset{k}{\mathbf{m}} - \frac{\partial\,\overset{k}{\mathbf{m}}}{\partial T_i}\cdot(K\,\overset{k}{\mathbf{c}} + \mu_0 M_s \mathbf{H}) \\ &\qquad + \frac{3}{2} c_0 \lambda_{100}\frac{\partial tr(\mathbf{T})}{\partial T_i} \\ &= \frac{\partial\,\overset{k}{\mathbf{m}}}{\partial T_i}\cdot\mathbf{K}\,\overset{k}{\mathbf{m}} + \frac{1}{2}\,\overset{k}{\mathbf{m}}\cdot\frac{\partial\mathbf{K}}{\partial T_i}\,\overset{k}{\mathbf{m}} - \frac{\partial\,\overset{k}{\mathbf{m}}}{\partial T_i}\cdot(\mathbf{K} - \overset{k}{\gamma}\,\mathbf{I})\,\overset{k}{\mathbf{m}} \\ &\qquad + \frac{3}{2} c_0 \lambda_{100}\frac{\partial tr(\mathbf{T})}{\partial T_i} \\ &= \frac{1}{2}\,\overset{k}{\mathbf{m}}\cdot\frac{\partial\mathbf{K}}{\partial T_i}\,\overset{k}{\mathbf{m}} + \frac{3}{2} c_0 \lambda_{100}\frac{\partial tr(\mathbf{T})}{\partial T_i} \\ &= -\left\{\begin{array}{ll} \frac{3}{2}\lambda_{100}(m_i^k m_i^k - c_0),\ i \in \{1,2,3\} & \\ 3\lambda_{111}\,\overset{k}{m}_1\overset{k}{m}_2, & i=4 \\ 3\lambda_{111}\,\overset{k}{m}_2\overset{k}{m}_3, & i=5 \\ 3\lambda_{111}\,\overset{k}{m}_3\overset{k}{m}_1, & i=6 \end{array}\right\} = -\,\overset{k}{\lambda}_i, \end{aligned} \tag{42}$$

where we use the identities

$$\frac{\partial\overset{k}{\mathbf{m}}}{\partial H_p}\cdot\overset{k}{\mathbf{m}} = 0,$$

$$\frac{\partial\overset{k}{\mathbf{m}}}{\partial T_i}\cdot\overset{k}{\mathbf{m}} = 0,$$

which originate from differentiating eq. (15b) with respect to field and stress.

Copyright © 2014 by ASME